Polymer 51 (2010) 2091–2098

Contents lists available at ScienceDirect

Polymer

journal homepage: www.elsevier.com/locate/polymer

Linear viscoelasticity of polymer blends with co-continuous morphology

Wei Yu*, Wei Zhou, Chixing Zhou

Advanced Rheology Institute, Department of Polymer Science and Engineering, Shanghai Jiao, Tong University, Shanghai 200240, China

ARTICLE INFO

Article history:
Received 15 November 2009
Received in revised form
2 February 2010
Accepted 1 March 2010
Available online 7 March 2010

Keywords:
Linear viscoelasticity
Polymer blend
Co-continuous morphology

ABSTRACT

The co-continuous morphology of polymer blends has received much attention not only because of its potential promotion of mechanical or electrical properties of polymer blends, but also due to its importance in phase separation by spinodal decomposition. Compared to the recent advances in the characterization of co-continuous structure, the rheology of co-continuous blends has not been understood clearly. In this work, a rheological model is suggested to correlate the linear viscoelasticity and the structural information of co-continuous blends. The dynamic modulus of co-continuous blends is composed of the contribution from components and the interface. The interfacial contribution, which is most important in the rheology of blends, is calculated from a simplified co-continuous structure. This model has been compared satisfactorily with available experimental results, which proves a reasonable connection between the co-continuous structure and linear viscoelasticity of blends.

1. Introduction

Blending polymers with different molecular structures or different mechanical properties has become a useful route in developing new, high-performance polymeric materials nowadays. Improved mechanical properties, processability, barrier behavior and electrical properties can be achieved through such technology. Choosing suitable polymers is of course the primary task in preparation of polymer blends, however, more attention has been paid to control the morphology of blends, which has been found to have a great impact on the properties of polymer blends. Actually, most polymers used in blends are immiscible or partially miscible due to their high molecular weight and unfavorable interactions, which result in the multiphase morphology. For binary polymer blends, when the content of one component is much lower than the other component, the minor component usually forms droplet in the matrix of major component, which is usually known as the sea-island morphology. The formation of droplet morphology [1], its dependence on the mixing condition and rheological properties [2], and the relationship between the droplet morphology and rheology [2–6] have been investigated thoroughly in recent years. When the content of minor component increases, it is possible that two components both forms a continuous network, which is known as the co-continuous morphology. It is well known that one of the purposes of blending is taking advantages of the component properties, and it has been found that co-continuous morphology sometime can supply a better combination of the component properties than the droplet morphology [7]. Besides mechanical properties, co-continuous morphology offers an opportunity to greatly decrease the conductive percolation concentration in carbon black filled composites [8]. Moreover, co-continuous morphology is often observed during phase separation of partially miscible polymer blends via spinodal decomposition [9]. Therefore, understanding the dynamics of morphology evolution and the relationship between the morphology and properties is not only a requirement to control the morphology in the development of new materials, but also the necessity to know the mechanism of polymer mixing and phase separation.

The investigations on co-continuous blends have been focused on the morphology determination [10–14], formation [15,16] and stability [17–21], mechanical properties [22–24] and rheological properties [25–31]. However, for a long time, the difficulty in the study of the co-continuous blend is the description of the morphology. The most frequently used method is the statistics on the interface due to its apparent irregularity. Theoretically, the area of interface per unit volume is used in modeling the evolution of interfacial shape [32,33], while interface per unit area of image (photos usually taken by scanning/transmission electron microscopy, SEM/TEM) is often used in experiments [11] since only two-dimensional cross section of blends can be observed in most experiments. Such description is based on the coarse grained statistics of the interface, and is useful in determination of the cocontinuity interval by image analysis [11] and modeling the dynamics of morphology evolution [32,33]. Although this description can be instructive in morphology, the detailed shape of interface can not be re-constructed due to lack of the local information of

* Corresponding author. Tel.: +86 21 54743275; fax: +86 21 54741297.
E-mail address: wyu@sjtu.edu.cn (W. Yu).

0032-3861/$ – see front matter © 2010 Elsevier Ltd. All rights reserved.
doi:10.1016/j.polymer.2010.03.005

interface, such as the local curvatures. Until recently, some improvements have been made in describing the interface in three-dimensional spaces. Technologies used to determine the morphology include the semiautomatic serial sectioning and reconstructing [34], Transmission electron microtomography (TEMT) [35], X-ray microtomography [13], X-ray phase tomography [36], three-dimensional nuclear magnetic resonance (NMR) imaging [37] and laser scanning confocal microscopy (LSCM) [14,38–40]. It is then possible to obtain the area average of the mean and Gauss curvatures of local interfaces, although incorporation such structural information in constitutive model is still a challenging work. On the other hand, the quantitative relation between the co-continuous morphology and the rheological properties is still missing. The rheological properties, especially the linear viscoelasticity, of co-continuous blend have been found to be very instructive in the determination of the phase morphology. For example, the storage modulus and complex viscosity at low frequencies will generally increase with the volume fraction of minor component, reach a maximum at certain concentration, and then decrease with the volume fraction which denotes a transition from droplet morphology to co-continuous morphology [29,30]. However, it is still difficult to predict the linear viscoelasticity of co-continuous blends. The models based on the area tensor [33] or interfacial tensor [32] are not satisfying due to lack of intrinsic length scale. Even the revisions [41,42] of these models are technically not suitable since the length scale introduced is based on droplet morphology. Moreover, lack of quantitative description on the linear viscoelasticity of co-continuous morphology also hinders our understanding on the mechanism of spinodal decomposition in phase separation. Rheology has been frequently used to determine the binodal and spinodal temperature in phase separation [9,43–45]. However, the transition point is empirically assigned to the phase separation temperature due to the lack of the interplay between the concentration fluctuation and the interface. Usually, Palierne model [46] is used to account for the interfacial contribution to rheology, but it is only applicable to droplet morphology generated during nucleation and growth in off-critical compositions and apparently not suitable for co-continuous morphology created during spinodal decomposition in near-critical blends.

In this paper, the linear viscoelasticity of polymer blends with co-continuous morphology will be modeled. The purpose is to establish a quantitative connection between the structural information of co-continuous morphology and the corresponding linear viscoelasticity.

2. Theoretical model

The dynamic modulus under small amplitude oscillatory shear flow will be considered here. It is assumed the co-continuous morphology will not change under sinusoidal shear strain with sufficient small strain asmplitude. Although some experiments have shown the possibility of coarsening [13] during annealing, the change of morphology will be ignored in the present work. This has been verified by almost collapsed dynamic modulus in repeated frequency sweep on the same sample. The complex modulus of co-continuous blends can be assumed to be a sum of components contribution and interface contribution, i.e.,

$$G^*_{\text{blend}} = G^*_{\text{components}} + G^*_{\text{interface}} \tag{1}$$

This is similar to the model of blends with droplet morphology [47], where the additivity comes from the separate contributions from the polymer components and the interface to the total free energy of the blends.

In modeling the rheological properties, the definition of co-continuous morphology in polymer blends is of critical importance. Generally, two main views have been reported in literature [16]. The classical one defines an ideal co-continuous morphology where at least two continuous structures exist in the same volume. The other one is based on the percolation threshold theory, and defines a co-continuous morphology as one in which at least a part of each phase forms a continuous structure that permeates the whole volume, which allows the existence of discrete domains that are not part of the network structure. When the concentration of one component increases, the morphology will gradually change from the droplet structure into a co-continuous structure of the second definition, i.e., a mixture of discrete droplet structure and a continuous network structure. An ideal co-continuous structure can be obtained when the concentration of minor component is sufficient high. These two definitions can be differentiated by the portion of a fully co-continuous structure, i.e., the continuity index [48]. The ideal continuous structure corresponds to the continuity index of 1, while the second definition of co-continuous structure generally covers a wider range of concentrations. Although the classical definition is a special case of the second definition, only the ideal co-continuous structure will be modeled here.

2.1. Components contribution

The most frequently used model for linear viscoelasticity of polymer blends is the Palierne model [46], from which the contribution of components can also be obtained under zero interfacial tension condition,

$$G^*_{\text{components}} = G^*_2 \frac{1+3\phi_1 H}{1-2\phi_1 H} \tag{2}$$

where $H = (G^*_1 - G^*_2)/(2G^*_1 + 3G^*_2)$. G^*_1 and G^*_2 are the complex modulus of fluid I and II, respectively. ϕ_1 is the volume fraction of fluid I. Palierne model has been used to predict the dynamic modulus of blends with droplet morphology. It is clear that exchanging two fluids in Eq. (3) will certainly cause a different complex modulus of blends. This suggests that Palierne model might be unsuitable for co-continuous blends.

The other model for the contribution from components in oscillatory shear has been suggested by Veenstra et al. [23] more recently. The original model was put forward to predict the mechanical properties of polymer blends with co-continuous morphology. A parallel model with series-linked parts and a series model with parallel-linked parts were derived for co-continuous blends. The parallel model was then extended to predict the complex modulus of co-continuous blends [28], where the Young's modulus in the original model was replaced by the dynamic complex modulus of components. It is assumed that the co-continuous morphology can be schematically shown in Fig. 1 a. The only important parameter is the volume fraction, and the length of the cell is normalized to 1. Therefore, no characteristic length is considered here. The complex modulus from the components of co-continuous blends can be expressed as [23,28]

$$G^*_{\text{components}} = \frac{a'^2 b' G^{*2}_1 + \left(a'^3 + 2a'b' + b'^3\right) G^*_1 G^*_2 + a' b'^2 G^{*2}_2}{b' G^*_1 + a' G^*_2} \tag{3}$$

where $\phi_1 = 3a'^2 - 2a'^3$ is the volume fraction of fluid I and $b' = 1 - a'$. It is noticed that Eq. (3) is symmetric for fluid I and II, which suggests that exchanging fluid I and fluid II will not change the complex modulus of blends. It should be stressed that the original Veenstra et al. model is sufficient for mechanical properties

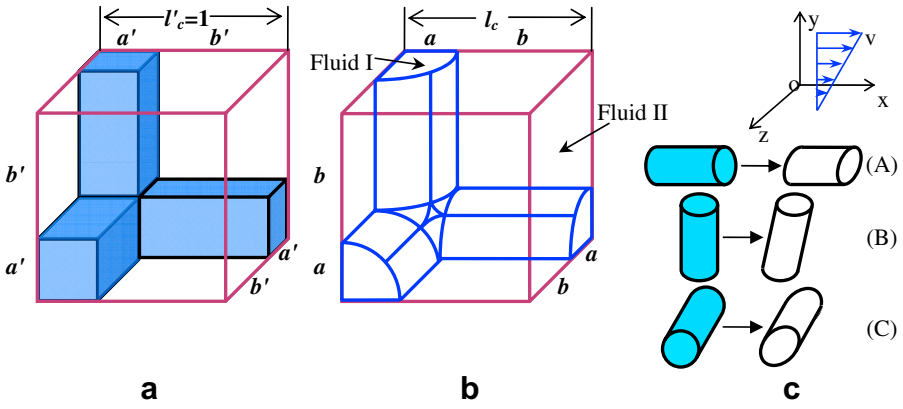

Fig. 1. Schematics of an ideal co-continuous morphology for (a) the components contribution, (b) the interfacial contribution and (c) deformation of interfaces.

since the interfacial would be unimportant in the prediction of mechanical properties. However, as will be shown below, it generally under-predicts the dynamic modulus of co-continuous blends due to the presence and deformation of interface under oscillatory shear flow.

2.2. Interfacial contribution

Extra contribution from interface can be determined from the deformation of interface. However, unlike the regular morphology with well defined structures, such as droplet morphology, modeling on the deformation of co-continuous structure is rather difficult. The structure suggested by Veenstra et al. [23] can serve as a good simplification of the real complex structure, although the components will never form a rectangular shape in the melt of polymer blends. The cross section of one continuous phase should be circular-like due to the effect of interfacial tension. Therefore, the morphology suggested by Veenstra et al. is modified and shown in Fig. 1 b, where the co-continuous morphological element is separated into three cylinders with same geometrical parameters but different orientation. This structure can be viewed as a repeated element of co-continuous structures. The whole co-continuous structure can be re-constructed by periodically duplicating the element shown in Fig. 1 b. This is a simple geometrical model which assumes the size of cylinders is the same. Actually, more complex morphology might exist in co-continuous blend, i.e., the cylinders could be distorted/oriented and the cylinders could be different in size in different directions. Although it is quite simple in geometry, it will be shown in the discussions that this model can fit the experimental results quite well for blends with a wide range of viscosity differences. It is straightforward to define the reduced length $a' = a/l_c$, $b' = b/l_c$, where l_c is the characteristic length of the co-continuous morphology, a and b are the radius and length of the cylinder, respectively. It is also straightforward to calculate the specific area as $S_V \equiv S/V = 3\pi ab/2l_c^3 = 3\pi a'b'/2l_c$.

Considering the orientation of cylinders, different behaviors of deformation can be observed under an oscillatory shear, and contribute differently to the dynamic rheological properties. Three typical forms of deformation can be expected and shown in Fig. 1 c (type A, B and C). The stress response under a specific flow field can be assumed to be the sum of the responses of these cylinders. The shear direction is along axis of the cylinder and the gradient direction along the cross section of the cylinder for type A, where both the interfacial area and the orientation of interface changes very slightly, and it is expected to contribute little to the stress of blend. The shear direction is along the cross section of the cylinder while the gradient direction along the axis of the cylinder for type B. The shape of the cross section of the cylinder remains circular. The stress response comes mainly from the tilt of the cylinder. Moreover, it is expected that the interfacial tension has little effect on the deformation in type B due to the constant cross sectional shape. It is reasonable to model the deformation of type B by an affine deformation model. The shear direction and the gradient direction are both perpendicular to the axis of the cylinder in type C. The shape of cross section becomes an ellipse with the length of cylinder unchanged. The stress response by type C deformation is mainly attributed to its deformed shape of cross section. It is also expected that the interfacial tension will play an important role, which is similar to the deformation of a spherical droplet in flow field.

2.2.1. Affine deformation for type A and B

It is assumed that the deformation and the interfacial stress can be described in a similar manner of infinite cylinder. Therefore, the morphology can be readily described by the area tensor, $A_{ij} = \frac{1}{V}\int_\Gamma n_i n_j dS$, which is anisotropic when the cylinder changes its orientation. The area tensors for cylinders with typical orientations are

$$A_{ij} = S'_V \begin{pmatrix} 0 & 0 & 0 \\ 0 & \frac{1}{2} & 0 \\ 0 & 0 & \frac{1}{2} \end{pmatrix} \text{ (type A)},$$
$$A_{ij} = S'_V \begin{pmatrix} \frac{1}{2} & 0 & 0 \\ 0 & 0 & 0 \\ 0 & 0 & \frac{1}{2} \end{pmatrix} \text{ (type B)} \quad (4)$$

where S'_V denotes the specific area of a cylinder, which is 1/3 of the specific area S_V of the co-continuous element shown in Fig. 1 b. The evolution of area tensor under flow field can be readily expressed as [33]

$$\dot{A}_{ij} + L_{ki}A_{kj} + A_{ik}L_{kj} - L_{kl}A_{klij} = 0 \quad (5)$$

where $L_{ij} = \partial v_i/\partial x_j$ defines the velocity gradient on the interface, and $A_{ijkl} = \frac{1}{V}\int_\Gamma n_i n_j n_k n_l dS$ is the fourth order area tensor. A closure approximation is necessary to solve the equation. A quadratic approximation is taken here, i.e., $A_{ijkl} = A_{ij}A_{kl}/S'_V$, which has also been used in Doi–Ohta model [32]. The most difficult one is the determination of the velocity gradient on the interface, which usually depends on the rheological properties of two components. However, only the simplest case is considered here, i.e., the interface will evolve passively or the so-called affine deformation is assumed here. So the velocity gradient is taken as the applied flow field. Considering the oscillatory shear flow with angular frequency ω and strain amplitude γ_0,

$$L_{ij} = \frac{\partial v_i}{\partial x_j} = \begin{pmatrix} 0 & \dot{\gamma} & 0 \\ 0 & 0 & 0 \\ 0 & 0 & 0 \end{pmatrix}, \gamma = \gamma_0 \sin(\omega t), \dot{\gamma} = \gamma_0 \omega \cos(\omega t) \quad (6)$$

the area tensor can be expanded to the first order of strain amplitude. The in-phase and out-phase of strain can be obtained from Eq. (5) and solved simultaneously to get the components of area tensor under oscillatory shear. The shear stress can be obtained from its 12 component. It is found that the stress contribution by type A deformation is zero, which agrees with our expectation. The interfacial stress due to type B deformation can be expressed as $\sigma^s_{12,B} = \frac{1}{2}\alpha S'_V \gamma = \frac{1}{6}\alpha S_V \gamma$, where α is the interfacial tension. It is clear that the stress $\sigma^s_{12,B}$ is in-phase of the applied strain. This suggests the interfacial contribution to the stress of type B deformation is purely elastic, which is consistent with the assumption of affine deformation. Therefore, the elastic modulus due to type B deformation can be expressed as $G'_{s,B} = \frac{1}{6}\alpha S_V$.

2.2.2. Non-affine deformation for type C

In type C deformation, only the cross section of the cylinder changes from a circle to an ellipse. A two-dimensional model can be used to describe such shape evolution. The ellipse is described by a shape tensor, which requires that all points x_i on the boundary of ellipse satisfies $G_{ij}x_i x_j = 1$. The shape tensor becomes a second rank unit tensor when the cross section becomes a circle. The evolution of shape tensor can be expressed as [49]

$$\frac{DG_{ij}}{Dt} + L_{ki}G_{kj} + G_{ik}L_{kj} = 0 \quad (7)$$

where D/Dt denotes materials derivatives. The velocity gradient tensor L_{ij} can be expressed in different ways [50]. The simplest one is that for Maffettone-Minale model [50,51], which is suggested for three-dimensional ellipsoidal shape. For two-dimensional deformation of a circular shape, the velocity gradient can be modified as

$$L_{ij} = \omega^A_{ij} + f_2 e^A_{ij} + \frac{f_1}{2\tau}\left(\frac{2G_{ij}}{G_{kk}} - \delta_{ij}\right) \quad (8)$$

where $\tau = \eta_m a/\alpha$, a being the radius of the initial circular shape, e_{ij} and ω_{ij} are the deformation rate tensor, $e_{ij}=(L_{ij} + L_{ji})/2$, and the vorticity tensor, $\omega_{ij}=(L_{ij} - L_{ji})/2$, of the applied flow field, respectively. e_{ij} with superscript A refers to the applied deformation rate, and e_{ij} without superscript is associated with the deformation of the droplet. f_1 and f_2 are given by:

$$f_1 = \frac{40(p+1)}{(2p+3)(19p+16)}, \quad f_2 = \frac{5}{2p+3} \quad (9)$$

p is the viscosity ratio between fluid I and II (Fig. 1 b).

The shape evolution under small amplitude oscillatory shear can be solved by series expansion of the dynamic equation, which has been done for three-dimensional drop [47]. Similar approach was taken here to get the shape of ellipse in oscillatory shear to the first order of strain amplitude, where the shape tensor can be written as

$$G_{ij} = \delta_{ij} + M_{ij}, \quad \delta_{ij} = \begin{pmatrix} 1 & 0 \\ 0 & 1 \end{pmatrix}, \quad M_{ij} = \begin{pmatrix} 0 & M_{12} \\ M_{12} & 0 \end{pmatrix},$$
$$M_{12} = k_s \sin(\omega t) + k_c \cos(\omega t) \quad (10)$$

where

$$k_s = -\frac{f_2\omega^2\tau^2}{f_1^2 + \omega^2\tau^2}\gamma_0, \quad k_c = -\frac{f_1 f_2 \omega\tau}{f_1^2 + \omega^2\tau^2}\gamma_0 \quad (11)$$

Therefore, the shape parameters of the ellipse can be determined from the eigenvalues of the shape tensor, i.e., the length of ellipse equal to the reciprocal of the square root of the eigenvalues, and the orientation angle of ellipse can be determined from the corresponding eigenvectors. The shear stress can be calculated by integration over the interface of the cylinder

$$\sigma^s_{12,C} = -\frac{\alpha}{V}\int_\Gamma n_1 n_2 dS = \frac{3\pi ab}{l_c^3}\alpha\gamma f_2 \omega\tau \frac{f_1\cos(\omega t) + \omega\tau\sin(\omega t)}{f_1^2 + \omega^2\tau^2} \quad (12)$$

which gives the dynamic modulus as

$$G'_{s,C} = \frac{3\pi ab}{16 l_c^3}\alpha\frac{f_2\omega^2\tau^2}{f_1^2 + \omega^2\tau^2} = \frac{1}{8}\alpha S_V \frac{f_2\omega^2\tau^2}{f_1^2 + \omega^2\tau^2} \quad (13)$$

$$G''_{s,C} = \frac{3\pi ab}{16 l_c^3}\alpha\frac{f_1 f_2\omega\tau}{f_1^2 + \omega^2\tau^2} = \frac{1}{8}\alpha S_V \frac{f_1 f_2\omega\tau}{f_1^2 + \omega^2\tau^2} \quad (14)$$

It is noticed that the dynamic modulus from type C deformation is a single mode Maxwell type model, which is similar to that of three-dimensional ellipsoidal drop with the difference in the coefficient and the dependence on volume fraction. Therefore, the dynamic modulus can be written as a sum of components contribution and the interface contribution, i.e.,

$$G' = G'_{\text{components}} + G'_s = G'_{\text{components}} + G'_{s,A} + G'_{s,B} + G'_{s,C}$$
$$= G'_{\text{components}} + \frac{k_C}{6}\alpha S_V\left(\frac{k_B}{k_C} + \frac{3}{4}\frac{f_2\omega^2\tau^2}{f_1^2 + \omega^2\tau^2}\right) \quad (15)$$

The above equations are obtained when the axis of cylinder is along the coordinate axis. Actually, the orientation of cylinder in a real co-continuous morphology could be random. Therefore, coefficients k_i are added before the interfacial contribution to account for the random orientation and possible distortion of co-continuous element, where the subscript B and C denotes the transformation of type B and type C structure. It can be readily proved by the orientation of coordinate that k_i is an order of unit. For isotropic blends, k_B and k_C should be of the same order and k_B/k_C is about one. However, if the co-continuous blends are subjected to shear or compression like flow (such as in compression molding in preparing sample for rheological measurements), the portion of type B structure that is still normal to the shear direction will decrease and k_B/k_C would become smaller than 1.

In the present model, the dynamic modulus of co-continuous blends can be well correlated with the morphology. Therefore, it might be useful to monitor the structural evolution of co-continuous blends via small oscillatory shear. This is important since the co-continuous morphology is not a rather stable structure, and will coarsen during annealing. On the other hand, the development of co-continuous morphology is often observed in the phase separation via spinodal decomposition mechanism. The time dependent of dynamic modulus under a specific frequency is often used to monitor the morphological evolution. It seems that the scaling relationship between the dynamic modulus and the characteristic length in morphology $G' \propto S_V^n$ is important here. It is clear from Eq. (15) that when the frequency is sufficient low, usually the interfacial contribution to the storage modulus will overtake the contribution of components, and the storage modulus is proportional to the specific area, i.e., $G' \propto S_V \propto l_c^{-1}$. However, as the frequency increases, the contribution from components increases. It is then not difficult to understand the finding of other scaling relations with n smaller than 1, for example, n is found to be 0.3 at 0.1 rad/s by Barron et al. [53]. Therefore, it is believed that instead of using

the scaling relationship $G' \propto S_V^n$ under a single frequency, a complete frequency dependency of dynamic modulus is necessary to obtain the reasonable structural information.

3. Comparisons with experiments

It is shown in Eq. (15) that the dynamic modulus of co-continuous blends can be quantitatively correlated with the characteristic length scale l_c. This is similar to the case of droplet structure, where the storage modulus at low frequency is determined by the ratio between the interfacial tension and the droplet radius. Such relationship has been used to quantitatively determine the rheology from morphological information and vice versa [47]. It is expected that such quantitative interconversion between rheology and morphology for co-continuous blend is also possible based on the above model. To show such connections, comparisons with the experimental data for different polymer blends will be shown.

3.1. Polystyrene/poly(ethylene-co-1-octene) blends

Model bends of polystyrene (PS, MC3700, Chevron Phillips Chemical Company, China, density 1.05 g/cm^3) and poly(ethylene-co-1-octene) (POE, 815A, DuPont & Dow Company, USA, density 0.868 g/cm^3) were prepared by melt mixing in an XSS-300 torque rheometer under 50 rpm at 180 °C for 10 min. A series of blends with compositions from 10/90 to 90/10 have been prepared. Rheological measurements for all blends were performed on a rotational rheometer (Bohlin Gemini 200HR, Malvern, UK) at 180 °C. Strain amplitude oscillatory sweep was first taken to determine the linear regime, and a frequency sweep with suitable strain amplitude in linear regime was performed with the frequency range 0.01–100 rad/s. The cocontinuity interval was determined by the maximum storage modulus at 0.01 rad/s as a function of composition [27,28], which is 40–60 wt% of POE. This range of co-continuous structure is justified by photos taken by scanning electron microscopy (SEM, type S-2150, Hitachi High-Technologies Corp. Japan). The interfacial tension between PS and POE was measured by droplet retraction method, and is about 2 mN/m at 180 °C [52]. Possible change of morphology during rheological measurement is excluded by the almost same frequency dependence of modulus taken before and after annealing the blends at 180 °C for 20 min.

The storage moduli of three blends are shown in Fig. 2. An enhanced elasticity at low frequency is obviously shown. It is clear that the slope of G′ at low frequency in log–log plot is significantly smaller than 2, which is the typical terminal slope of linear polymers. Moreover, it is also different from the shoulder-like behavior at low frequency of immiscible blends with droplet morphology. Actually, the shoulder in G′ of blend with droplet morphology represents an additional relaxation due to the deformation of droplet, and terminal slope of 2 will appear at lower frequency. However, the storage modulus does not show the terminal slope of 2 in the present experiments and also in many other experiments. One possibility is that the terminal behavior will appear at very low frequency which is not accessible in almost all experiments. The other possibility is there will be no terminal slope of 2 even at the vanishing frequency. This experimental observation is consistent with the present model, which suggests that the dynamic modulus is contributed from the deformation of element cylinders with different orientations. No matter what the orientation of element cylinders are, there is always a possibility to have a portion of structure that only contributes to the elastic modulus of the blend, such as the type B in ideal morphology as shown in Fig. 1 c.

To verify the present model quantitatively, the storage modulus of the blends are fitted with the characteristic length l_c as a fitting parameter (Fig. 2). The ratio of k_B/k_C is taken to be one. Keeping in mind that k_B and k_C represent an average effect of orientation and distortion of co-continuous element. The predictions of the model by Veenstra et al. [23] are also shown in Fig. 2 as dash lines, which are very close to the experiments at high frequencies since only the contribution of components is important there. It should be stressed here that the square columns/rods morphology assumed in the

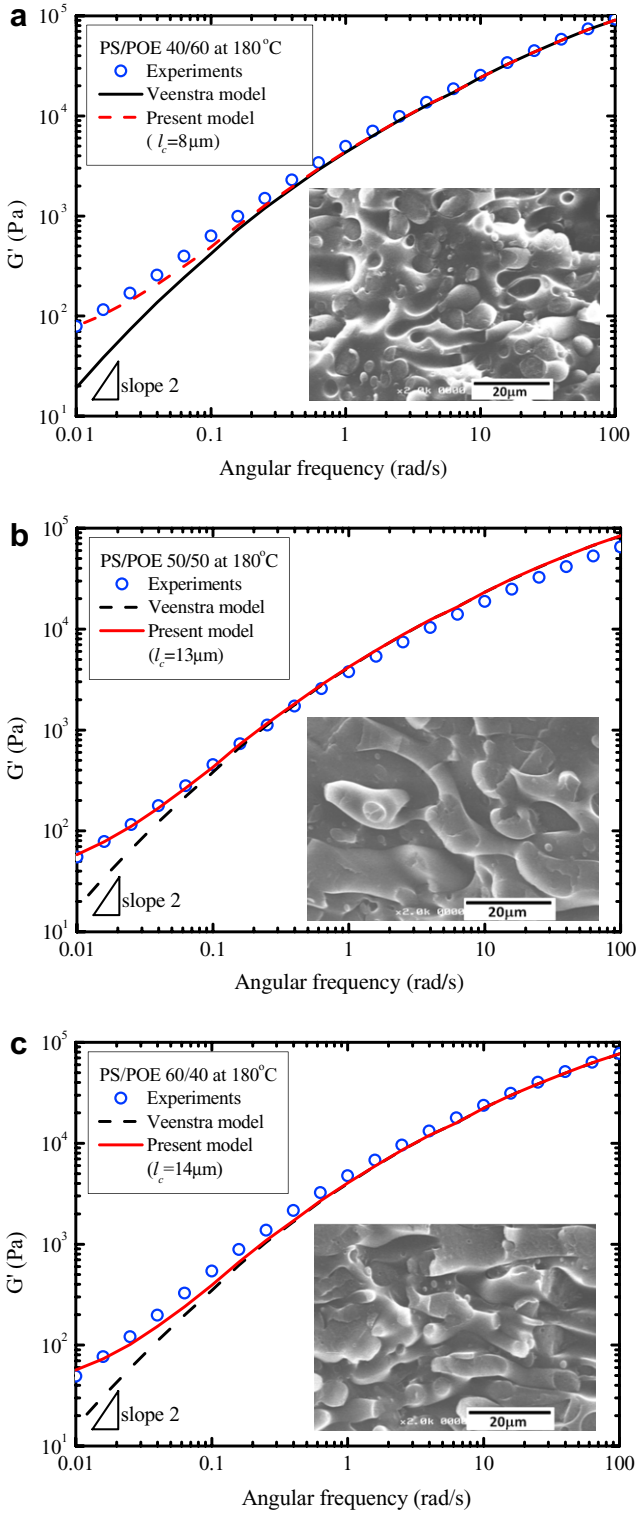

Fig. 2. Storage modulus of PS/POE co-continuous blends as a function of frequency. (a) PS/POE 40/60; (b) PS/POE 50/50; (c) PS/POE 60/40. Insets are the corresponding SEM pictures.

Veenstra model is substantially different from that in experiments which often takes irregular shape with circular cross section. However, the agreement of the Veenstra model at high frequencies with the experiments suggests that the details of morphology might be not so important when the interfacial tension is neglected. Moreover, it is also evident that Veenstra et al. model under-predicts the storage modulus at low frequency since no interfacial contribution is considered. The present model takes the Veenstra et al. model as the contribution of components with the modification of interfacial contribution. Therefore, prediction at high frequency is the same as that of Veenstra et al. model. At low frequency, the present model catches the trend of storage model satisfactorily with suitable choice of characteristic length l_c. The SEM pictures of the morphology of blends are also shown as insets in the plots. Evaluation of l_c from SEM is not straightforward since the SEM pictures show irregular shape of morphology in most cases. Moreover, determination of the true characteristic length requires a three-dimensional structure due to the possible orientation and distortion of cylinders. If only two-dimensional pictures are available, l_c is estimated to be a half of the sum of the mean cylinder diameter and the mean distance between cylinders. It is interesting to find that the characteristic lengths used in the model prediction are quite close to that shown in the SEM pictures. This manifests that the quantitative connection between the co-continuous morphology and the rheology can be well established by the present model.

3.2. Other blends in literature

Barron and Macosko [53] reported recently a morphological and rheological study of co-continuous blends of polystyrene (PS) and acrylonitrile-styrene copolymer with 20% mol acrylonitrile (SAN). The zero shear viscosities of PS and SAN20 are 1500 Pa s and 2300 Pa s, respectively. The morphology was determined by laser scanning confocal microscopy, from which the geometrical parameters like interfacial area per unit volume and area average absolute curvature and Gaussian curvature can be obtained. The predictions of present model and Veenstra et al. model are shown in Fig. 3, with an inset of a 3D reconstruction of co-continuous structure of PS/SAN blend observed by LSCM [53]. As it has been shown above, Veenstra et al. model only works well at high frequency, where the interfacial contribution is irrelevant. The predictions of present model (solid line and dash-dot line in Fig. 3)

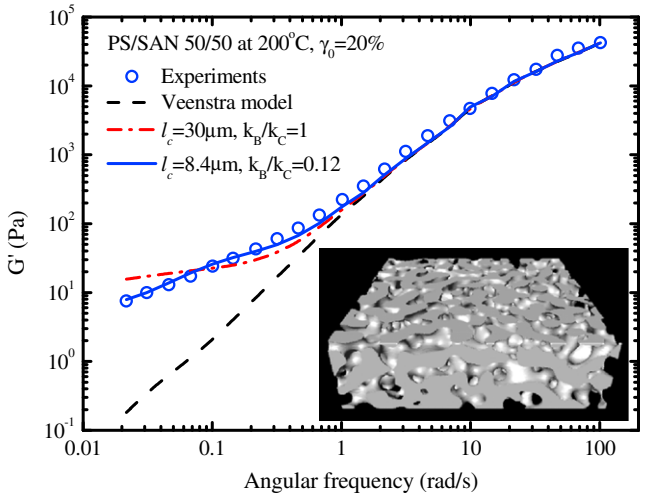

Fig. 3. Storage modulus of PS/SAN co-continuous blends as a function of frequency. Inset is the corresponding three-dimensional morphology after annealing 5 min at 200 °C [53]. The volume of the image is 150 × 158 × 46.5 μm^3.

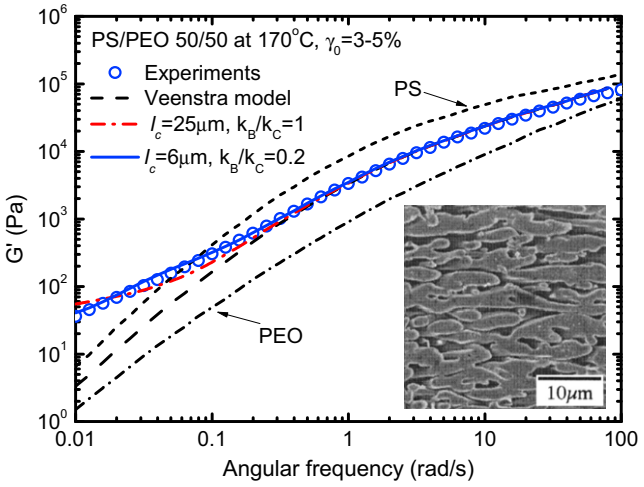

Fig. 4. Storage modulus of 50/50 POE/PS blend with co-continuous morphology. Inset is the corresponding SEM picture with PEO removed by water extraction [54].

agree the general trend of experiments. If the blend is assumed to be isotropic, i.e., $k_B/k_C = 1$, the best fit (dash-dot line) gives characteristic length about 30 μm, but the frequency dependence at low frequency is not well modeled. This discrepancy is ascribed to the non-ideal co-continuous morphology due to rotation and distortion of the ideal co-continuous structure. In the blends, it is possible that the element cylinders (A, B and C in Fig. 1 c) do not have the same volume fraction and are not orthogonal. Moreover, in a non-ideal co-continuous morphology, it is possible to have discrete droplet structure, which makes the blends relax faster due to its relatively short relaxation time. Although the characteristic length used in the model ($l_c = 30$ μm) seems consistent apparently with direct the morphology observation (from the front view with the height of 46.5 μm), it is much larger than that estimated from the area per unit volume. It is shown that the specific area is about 0.14 μm^{-1} [53], which corresponds to the characteristic length 8.4 μm. Therefore, the best fit with experimental data gives $k_B/k_C = 0.12$, which implies only a small portion of type B structure effectively exist in the blends and a strong distortion/orientation of the co-continuous morphology in shear-velocity gradient plane. Validation of this conclusion needs further experiments on the morphology during rheological measurement, which is unavailable in literature now.

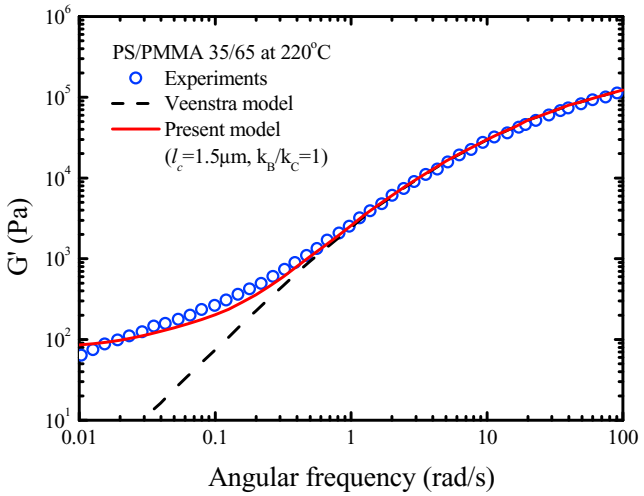

Fig. 5. Storage modulus of 35/65 PS/PMMA blend at 220 °C.

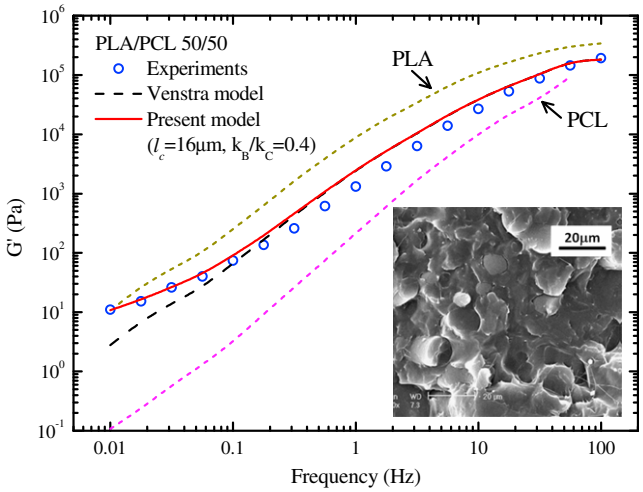

Fig. 6. Storage modulus of 50/50 PLA/PCL blend with co-continuous morphology. Inset is the corresponding SEM picture [58].

Galloway and Macosko investigated the detection of cocontinuity in poly(ethylene oxide)/polystyrene (PEO/PS) blends [54]. The co-continuous morphology of POE/PS blends were determined by several methods including the rheological methods. As an example, the storage modulus of typical co-continuous morphology (50/50 blend) is shown in Fig. 4. G′ of blends at high frequency is between that of two components. The present model also give quite satisfactory prediction on G′ with the interfacial tension 3.9 mN/m [55]. Especially, if the anisotropy of co-continuous structure is considered ($k_B/k_C = 0.2$), the best fit gives a characteristic length 6 μm, which is well consistent with the direct morphology observation (see inset of Fig. 4).

Bell investigated the blends of polystyrene and poly(methyl methacrylate) (PS/PMMA) [56]. Study on the continuity reveals that blends with PS content between 35wt% and 55wt% show co-continuous morphology. The storage modulus of 35/65 PS/PMMA blend is shown in Fig. 5. The interfacial tension between PS and PMMA is 0.6 mN/m at 220 °C [57]. It is shown that present model with characteristic length 1.5 μm gives a reasonable prediction on the storage modulus. The deviations here could be attributed to the non-ideal co-continuous morphology. Actually, blend with 35wt% PS is the boundary of cocontinuity interval. The continuity index of PS is only 0.25, which suggests that a lot of the PS is dispersed as droplets and only a portion of the PS domains forms a percolation network.

Wu et al. [58] investigated the morphology and rheology of the blends of polylactide and poly(ϵ-caprolactone). The storage modulus of 50/50 blend is shown in Fig. 6, which exhibits a co-continuous structure as seen from the SEM pictures (inset of Fig. 6). The storage modulus is also fitted by the present model with the interfacial tension 1.5 mN/m, which is determined by fitting with the dynamic modulus for 80/20 and 20/80 blends with Palierne model. The model of Veenstra et al. (dash line in Fig. 6) shows only the contribution of components, and is consistent with the experiments only at high frequency. The prediction of present model with $l_c = 16$ μm and $k_B/k_C = 0.4$ fits quite well with experiments.

4. Conclusions

A new model is suggested in the work to describe the linear viscoelasticity of polymer blends with co-continuous morphology. It has been shown that the interfacial contribution to the dynamic modulus is quite important at low oscillatory frequency, and the characteristic length in this model is well correlated with morphological information determined using electron microscopy. It is found that two types of element structures play an important role in the terminal behavior. Moreover, it is found that the present model works well for blends with a wide range of viscosity differences. The viscosity ratios for all the blends tested here range from 1 (PS/PMMA) to about 16 (PLA/PCL), which proves the wide applicability of the present model in polymer blends.

Acknowledgement

This work is supported by Natural Science Foundation of China (No. 50930002, No. 20674051). This work is also partly supported by Shanghai Leading Academic Discipline Project (No. B202). W. Y. is supported by the SMC project of Shanghai Jiao Tong University.

References

[1] Yu W, Zhou CX. J Rheol 2007;51:179–94.
[2] Tucker III CL, Moldenaers P. Annu Rev Fluid Mech 2002;34:177–210.
[3] Yu W, Bousmina M, Grmela M, Palierne JF, Zhou CX. J Rheol 2002;46:1381–99.
[4] Yu W, Zhou CX, Bousmina M. J Rheol 2005;49:215–36.
[5] Yu W, Bousmina M, Zhou CX. J Non-Newtonian Fluid Mech 2006;133:57–62.
[6] Briscoe BJ, Lawrence CJ, Mietus WGP. Adv in Colloid & Interface Sci 1999;81:1–17.
[7] Utracki LA. Commercial polymer blends. London: Chapman & Hall; 1998. p. 98.
[8] Zhou P, Yu W, Zhou CX, Liu F, Hou LM, Wang J. J Appl Polym Sci 2007;103:487–92.
[9] Zhang RY, Cheng H, Zhang CG, Sun TC, Dong X, Han CC. Macromolecules 2008;41:6818–29.
[10] Li J, Favis BD. Polymer 2001;42:5047–53.
[11] Galloway JA, Montminy MD, Macosko CW. Polymer 2002;43:4715–22.
[12] Omonov TS, Harrats C, Moldenaers P, Groeninckx G. Polymer 2007;48:5917–27.
[13] Pyun A, Bell JR, Won KH, Weon BM, Seol SK, Je JH, et al. Macromolecules 2007;40:2029–35.
[14] Lopez-Barron C, Macosko CW. Langmuir 2009;25:9392–404.
[15] Marin N, Favis BD. Polymer 2002;43:4723–31.
[16] Pötschke P, Paul DR. J Macromol Sci Part C Polym Reviews 2003;43:87–141.
[17] Willemse RC. Polymer 1999;40:2175–8.
[18] Lee JK, Han CD. Polymer 1999;40:2521–36.
[19] Willemse RC, de Boer AP, van Dam J, Gotsis AD. Polymer 1999;40:827–34.
[20] Veenstra H, Norder B, van Dam J, de Boer AP. Polymer 1999;40:5223–6.
[21] Veenstra H, van Dam J, de Boer AP. Polymer 2000;41:3037–45.
[22] Willemse RC, Speijer A, Langeraar AE, de Boer AP. Polymer 1999;40:6645–50.
[23] Veenstra H, Verkooijen PCJ, van Lent BJJ, van Dam J, de Boer AP, Nijhof APHJ. Polymer 2000;41:1817–26.
[24] Inberg JPF, Gaymans FJ. Polymer 2002;43:4197–205.
[25] Weis C, Leukel J, Borkenstein K, Maier D, Gronski W, Friedrich C, et al. Polym Bulletin 1998;40:235–41.
[26] Vinckier I, Laun HM. J Rheol 2001;45:1373–85.
[27] Steinmann S, Gronski W, Friedrich C. Rheol Acta 2002;41:77–86.
[28] Sengers WGF, Sengupta P, Noordermeer JWM, Picken SJ, Gotsis AD. Polymer 2004;45:8881–91.
[29] Castro M, Prochazka F, Carrot C. J Rheol 2005;49:149–60.
[30] Castro M, Carrot C, Prochazka F. Polymer 2004;45:4095–104.
[31] Filippone G, Dintcheva NT, Acierno D, La Mantia FP. Polymer 2008;49:1312–22.
[32] Doi M, Ohta T. J Chem Phys 1991;95:1242–8.
[33] Wetzel ED, Tucker III CL. Int J Multiphase Flow 1999;25:35–61.
[34] Alkemper J, Voorhees PW. J Microsc 2001;201:388–94.
[35] Sengupta P, Noordermeer JWM. Macromol Rapid Commun 2005;26:542–7.
[36] Momose A, Fujii A, Kadowaki H, Jinnai H. Macromolecules 2005;38:7197–200.
[37] Koizumi S, Yamane Y, Kuroki S, Ando I, Nishikawa Y, Jinnai H. J Appl Polym Sci 2007;103:470–5.
[38] Verhoogt H, Dam JV, de Boer AP, Draaijer A, Houpt PM. Polymer 1993;34:1325–9.
[39] Nishikawa Y, Koga T, Hashimoto T, Jinnai H. Langmuir 2001;17:3254–65.
[40] Nishikawa Y, Jinnai H, Koga T, Hashimoto T, Hyde ST. Langmuir 1998;14:1242–9.
[41] Lee HM, Park OO. J Rheol 1994;38:1405–25.
[42] Zhou CX, Yu W, Zhao DL. Canadian J Chem Eng 2003;81:1067–74.
[43] Kapnistos M, Hinrichs A, Vlassopoulos D, Anastasiadis SH, Stammer A, Wolf BA. Macromolecules 1996;29:7155–63.
[44] Vlassopoulos D, Koumoutsakos A, Anastasiadis SH, Hatzikiriakos SG, Englezos P. J Rheol 1997;41:739–55.
[45] Li RM, Yu W, Zhou CX. Polym Bulletin 2006;56:455–66.
[46] Palierne JF. Rheol Acta 1990;29:204–14.
[47] Yu W, Bousmina M, Grmela M, Zhou CX. J Rheol 2002;46:1401–18.
[48] Lyngaae-Jorgensen J, Rasmussen KL, Chtcherbakova EA, Ultracki LA. Polym Eng Sci 1999;39:1060–71.
[49] Wetzel ED, Tucker III CL. J Non-Newtonian Fluid Mech 2001;101:21–41.

[50] Yu W, Bousmina M. J Rheol 2003;47:1011–39.
[51] Maffettone PL, Minale M. J Non-Newton Fluid Mech 1998;78:227–41.
[52] Yang K. Rheological study of metallocene catalyzed poly(ethylene-1-octene). Master thesis. Shanghai Jiao Tong University; 2007.
[53] Barron CRL, Macosko CW. The XVth International Congress on Rheology 2008; 523–525.
[54] Galloway JA, Macosko CW. Polym Eng Sci 2004;44:714–27.
[55] Moriya S, Kawamoto S, Urakawa O, Adachi K. Polymer 2006;47:6236–42.
[56] Bell JR. Cocontinuous polymer blends: the role of block copolymer in blend morphology evolution. Ph. D thesis, The University of Minnesota, 2007.
[57] Mo HY, Zhou CX, Yu W. J Non-Newtonian Fluid Mech 2000;91:221–32.
[58] Wu DF, Zhang Y, Zhang M, Zhou W. European Polym J 2008;44:2171–83.